

SHIELDING AGAINST NEUTRONS FROM 400 MEV PROTON BEAMS

Radiation Physics Note 82
Alex Elwyn
November 1989

INTRODUCTION

Calculations of the attenuation of dose equivalent in concrete for neutrons produced in reactions of 150, 200, and 250 MeV protons striking a thick Fe target are described by Hagen, et al. in a SAIC Report (1). Freeman (2), in a determination of the shielding requirements for the Loma Linda accelerator in IB 1, has reviewed the SAIC procedures and parameterized their results with a simple exponential expression with two fit parameters. The present note describes an estimation of the neutron dose (really dose equivalent) attenuation for 400 MeV protons by a linear extrapolation of these parameters for each of the six angular bins in the SAIC report. These results can provide at least preliminary estimates of the shielding necessary for the Fermilab Linac upgrade to 400 MeV. They are also compared to calculations based on the semiphenomenological Moyer model (3).

PROCEDURE

The analytic expression developed by Freeman (2) to represent the SAIC dose attenuation calculations is

$$r^2 \times \text{DOSE}(\theta, i) = A_i(\theta) \times 10^{B_i(\theta)R}, \quad (1)$$

where r is the distance from the point source to the position of interest on the shield surface, R is the depth in the shield along the direction of interest θ , the angle relative to the incident beam direction, and i is an index that denotes the incident proton energy. For a spherical concrete shield completely surrounding the loss point $r=R$. For a non-zero distance d from the loss point to the shield surface $r = R + d$. The normalization constant $A_i(\theta)$ and the slope parameter $B_i(\theta)$ were parameterized as

$$\begin{aligned} A_i(\theta) &= a_i \times 10^{k_i \theta} \\ B_i(\theta) &= b_i + c_i \theta + d_i \theta^2. \end{aligned} \quad (2)$$

To estimate the dose at 400 MeV, an effective angle θ_e was determined from $\cos \theta_e = 0.5 \times (\cos \theta_i + \cos \theta_f)$ for each angular bin, where θ_i , θ_f are the bin limits. $A_i(\theta_e)$ and $B_i(\theta_e)$ calculated at each energy - 150, 200, and 250 MeV - were fit to a straight line and linearly extrapolated to 400 MeV for each effective angle separately. The values of the parameters at 400 MeV are displayed in Table 1. The straight line fits are shown in Figs. 1 and 2.

Following Freeman (2), the $A_i(\theta)$ and $B_i(\theta)$ values at $i=400$ MeV were parametrized as indicated in Eq. 2. The constants resulting from the fitting procedure are shown in Table 2 along with those at 150, 200, and 250 MeV from Table A.1 of Ref. (2). The 400 MeV fits are displayed in Fig. 3.

With $A_i(\theta_e)$ and $B_i(\theta_e)$ given in Table 1, values of $r^2 \times \text{DOSE}$ at 400 MeV were calculated as a function of R , the depth in the concrete shield, and are shown in Table 3 and plotted in Fig. 4 for each angular bin. For cases where the distance d is non-zero, the dose is given by

$$\text{DOSE } (\theta) = \frac{A(\theta) \times 10^{B(\theta)R}}{(d+R)^2} \quad (3)$$

Note that R is a function of t , the transverse shield thickness, and θ . Freeman (2) considers two basic shielding geometries - the side-wall and end-wall cases - and Ref. (2) should be consulted for specific shielding determinations. (See, for example, Fig. 7 and the discussion on p. 2 of Ref. (2)).

DISCUSSION

It is of interest to compare the 400 MeV dose values estimated from the SAIC calculations with those based on the semi-empirical model developed by Moyer (3) to determine transverse shield thicknesses for high-energy particle accelerators. As discussed by, for example, Stevenson, et al. (4) and McGaslin, et al. (5), the Moyer model expresses the dose equivalent at some point on a shield surface from a point-like loss of the proton beam as

$$r^2 \times H(\theta) = h \times e^{-\beta\theta} \times e^{-R/\lambda}, \quad (4)$$

where, based on high-energy experiments, $h = 2.84 \times 10^{-7} \times E^{0.8}$ Rem-cm² when E is in GeV. The neutron attenuation length in the shield, λ , is assumed independent of energy for high-energy particles (greater than 150 MeV) as is the angular distribution parameter β . For earth or concrete $\lambda = 117$ g/cm², and $\beta = 2.3$ rad⁻¹ for all energies and target materials. If t is the transverse shield thickness, R (in Eq. 4) = $t \times \csc \theta$. The Moyer model should only be used to estimate side-shielding (transverse) dose attenuation with θ restricted to $\pi/3 < \theta < 2\pi/3$.

Calculations of $r^2 \times \text{DOSE}$ as given in Eq. 4 were performed as a function of depth R in a concrete shield (density = 2.35 g/cm³). In Fig. 5 the Moyer model results at 400 MeV are compared to those extrapolated from the SAIC calculations. As observed, the two calculations are in good agreement particularly in those angular intervals for which the Moyer model was developed. Thus, the Moyer model provides a method for rapid estimation of transverse shielding even at energies as low as 400 MeV.

SUMMARY

The SAIC calculations extrapolated to 400 MeV can be used to estimate both side-wall and end-wall shielding requirements. For transverse shielding cases (i.e., angles near 90 degrees) the Moyer model can be a more rapid estimator. A complete calculation based on a sophisticated high-energy production and transport code, such as HETC (6), should be performed for 400 MeV protons to check the extrapolation procedure described here.

REFERENCES

1. W.K. Hagen, B.L. Colburn, T.W. Armstrong, "Radiation Shielding Calculations for the Loma Linda Proton Therapy Facility," SAIC Report #87/1072 (June, 1987).
2. W.S. Freeman, "Shield Walls in IB 1 for Loma Linda Accelerator," FNAL Radiation Physics Note #71 (May, 1988).
3. B.J. Moyer, "Evaluation of Shielding Required for the Improved Bevatron," LBL Report #UCRL-9769 (1961); B.J. Moyer, "Method of Calculation of the Shielding Enclosure for the Berkeley Bevatron," in: Proc. 1st Int. Conf. Shielding Around High Energy Accelerators, Presses Universitaires de France, p. 65 (1962).
4. G.R. Stevenson, Liu Kuei-Lin, R.H. Thomas, "Determination of Transverse Shielding for Proton Accelerators Using the Moyer Model," Health Physics 43, 13 (1982).
5. J.B. McCaslin, W.P. Swanson, and R.H. Thomas, "Moyer Model Approximations for Point and Extended Beam Losses," Nucl. Instru. & Meth. in Phys. Res. A256, 418 (1987).
6. T.W. Armstrong, K.C. Chandler, "The High Energy Transport Code HETC," Nucl. Sci. Engr. 49, 110 (1972).

TABLE 1: Values of the parameters of Eq. 1 at 400 MeV based on a linear fit to the values at 150, 200, and 250 MeV.

Ang. Range (Deg)	Eff. Angle, θ_e (Deg)	$A(\theta_e)$ (Rem-cm ² proton ⁻¹)	$B(\theta_e)$ (cm ⁻¹)
0-15	10.59	5.005 E-08	-0.0062
15-30	23.655	2.753 E-08	-0.0066
30-45	38.13	1.416 E-08	-0.0071
45-60	52.875	7.184 E-09	-0.0075
60-90	75.52	2.524 E-09	-0.0081
90-180	120.00	3.205 E-10	-0.0088

TABLE 2: Values of the fit parameters from a parameterization of the $A_i(\theta)$ and $B_i(\theta)$ as indicated in Eq. 2.

Energy (Mev)	a_i (cm ² Rem-prot ⁻¹)	k_i (deg ⁻¹)	b_i (cm ⁻¹)	c_i (cm ⁻¹ deg ⁻¹)	d_i (cm ⁻¹ deg ⁻²)
150	1.711 E-08	-0.0229	-0.0104	-5.148 E-05	2.155 E-08
200	2.921 E-08	-0.0216	-0.0091	-5.575 E-05	9.974 E-08
250	4.283 E-08	-0.0205	-0.0086	-4.554 E-05	4.978 E-08
400	8.215 E-08	-0.02005	-0.0058	-3.888 E-05	1.122 E-07

TABLE 3: Values of $r^2 \times \text{DOSE}$ at 400
 MeV in units of Rem cm⁻²
 proton⁻¹ as function of depth
 in concrete shield for various
 angular intervals

	A	B	C	D	E	F	G	H
1	R (cm)	0-150E	15-30DEG	30-45DEG	45-60DEG	60-90DEG	90-180DEG	
2	100	1.209E-08	5.981E-09	2.768E-09	1.275E-09	3.937E-10	4.205E-11	
3	110	1.049E-08	5.134E-09	2.351E-09	1.072E-09	3.269E-10	3.432E-11	
4	120	9.100E-09	4.407E-09	1.997E-09	9.020E-10	2.715E-10	2.802E-11	
5	130	7.895E-09	3.783E-09	1.696E-09	7.587E-10	2.254E-10	2.287E-11	
6	140	6.849E-09	3.248E-09	1.441E-09	6.382E-10	1.872E-10	1.866E-11	
7	150	5.942E-09	2.788E-09	1.224E-09	5.369E-10	1.555E-10	1.523E-11	
8	160	5.155E-09	2.393E-09	1.039E-09	4.516E-10	1.291E-10	1.243E-11	
9	170	4.472E-09	2.054E-09	8.827E-10	3.799E-10	1.072E-10	1.015E-11	
10	180	3.880E-09	1.764E-09	7.498E-10	3.196E-10	8.903E-11	8.283E-12	
11	190	3.366E-09	1.514E-09	6.368E-10	2.688E-10	7.393E-11	6.761E-12	
12	200	2.920E-09	1.300E-09	5.409E-10	2.261E-10	6.139E-11	5.518E-12	
13	210	2.534E-09	1.116E-09	4.594E-10	1.902E-10	5.098E-11	4.504E-12	
14	220	2.198E-09	9.576E-10	3.902E-10	1.600E-10	4.234E-11	3.676E-12	
15	230	1.907E-09	8.220E-10	3.315E-10	1.346E-10	3.516E-11	3.001E-12	
16	240	1.654E-09	7.056E-10	2.815E-10	1.132E-10	2.920E-11	2.449E-12	
17	250	1.435E-09	6.057E-10	2.391E-10	9.525E-11	2.424E-11	1.999E-12	
18	260	1.245E-09	5.200E-10	2.031E-10	8.013E-11	2.013E-11	1.632E-12	
19	270	1.080E-09	4.464E-10	1.725E-10	6.740E-11	1.672E-11	1.332E-12	
20	280	9.372E-10	3.832E-10	1.465E-10	5.670E-11	1.388E-11	1.087E-12	
21	290	8.131E-10	3.289E-10	1.245E-10	4.770E-11	1.153E-11	8.872E-13	
22	300	7.054E-10	2.823E-10	1.057E-10	4.012E-11	9.574E-12	7.241E-13	
23	310	6.120E-10	2.424E-10	8.979E-11	3.375E-11	7.951E-12	5.910E-13	
24	320	5.309E-10	2.081E-10	7.626E-11	2.839E-11	6.603E-12	4.824E-13	
25	330	4.606E-10	1.786E-10	6.478E-11	2.388E-11	5.483E-12	3.937E-13	
26	340	3.996E-10	1.533E-10	5.502E-11	2.009E-11	4.553E-12	3.214E-13	
27	350	3.467E-10	1.316E-10	4.673E-11	1.690E-11	3.781E-12	2.623E-13	
28	360	3.008E-10	1.130E-10	3.969E-11	1.422E-11	3.140E-12	2.141E-13	
29	370	2.609E-10	9.698E-11	3.371E-11	1.196E-11	2.607E-12	1.747E-13	
30	380	2.264E-10	8.325E-11	2.864E-11	1.006E-11	2.165E-12	1.426E-13	
31	390	1.964E-10	7.146E-11	2.432E-11	8.462E-12	1.798E-12	1.164E-13	
32	400	1.704E-10	6.135E-11	2.066E-11	7.118E-12	1.493E-12	9.502E-14	
33	410	1.478E-10	5.266E-11	1.755E-11	5.988E-12	1.240E-12	7.755E-14	
34	420	1.282E-10	4.520E-11	1.490E-11	5.037E-12	1.030E-12	6.330E-14	
35	430	1.113E-10	3.880E-11	1.266E-11	4.237E-12	8.551E-13	5.167E-14	
36	440	9.652E-11	3.331E-11	1.075E-11	3.564E-12	7.101E-13	4.217E-14	
37	450	8.374E-11	2.859E-11	9.133E-12	2.998E-12	5.897E-13	3.442E-14	
38	460	7.265E-11	2.455E-11	7.757E-12	2.522E-12	4.897E-13	2.809E-14	
39	470	6.303E-11	2.107E-11	6.589E-12	2.122E-12	4.066E-13	2.293E-14	
40	480	5.468E-11	1.809E-11	5.597E-12	1.785E-12	3.377E-13	1.872E-14	
41	490	4.744E-11	1.553E-11	4.754E-12	1.501E-12	2.804E-13	1.528E-14	
42	500	4.116E-11	1.333E-11	4.038E-12	1.263E-12	2.329E-13	1.247E-14	
43	510	3.571E-11	1.144E-11	3.429E-12	1.062E-12	1.934E-13	1.018E-14	
44	520	3.098E-11	9.822E-12	2.913E-12	8.937E-13	1.606E-13	8.306E-15	
45	530	2.687E-11	8.431E-12	2.474E-12	7.518E-13	1.334E-13	6.780E-15	
46	540	2.332E-11	7.237E-12	2.101E-12	6.324E-13	1.107E-13	5.534E-15	
47	550	2.023E-11	6.213E-12	1.785E-12	5.320E-13	9.196E-14	4.516E-15	
48	560	1.755E-11	5.333E-12	1.516E-12	4.475E-13	7.637E-14	3.686E-15	

	A	B	C	D	E	F	G	H
49	570	1.522E-11	4.578E-12	1.288E-12	3.764E-13	6.342E-14	3.009E-15	
50	580	1.321E-11	3.930E-12	1.094E-12	3.167E-13	5.266E-14	2.456E-15	
51	590	1.146E-11	3.374E-12	9.290E-13	2.664E-13	4.373E-14	2.004E-15	
52	600	9.941E-12	2.896E-12	7.891E-13	2.241E-13	3.632E-14	1.636E-15	
53	610	8.625E-12	2.486E-12	6.702E-13	1.885E-13	3.016E-14	1.335E-15	
54	620	7.482E-12	2.134E-12	5.693E-13	1.586E-13	2.504E-14	1.090E-15	
55	630	6.491E-12	1.832E-12	4.835E-13	1.334E-13	2.080E-14	8.896E-16	
56	640	5.632E-12	1.572E-12	4.107E-13	1.122E-13	1.727E-14	7.261E-16	
57	650	4.886E-12	1.350E-12	3.488E-13	9.438E-14	1.434E-14	5.927E-16	
58	660	4.239E-12	1.159E-12	2.963E-13	7.939E-14	1.191E-14	4.837E-16	
59	670	3.677E-12	9.947E-13	2.517E-13	6.679E-14	9.890E-15	3.948E-16	
60	680	3.190E-12	8.539E-13	2.138E-13	5.618E-14	8.213E-15	3.223E-16	
61	690	2.768E-12	7.330E-13	1.816E-13	4.726E-14	6.820E-15	2.630E-16	
62	700	2.401E-12	6.292E-13	1.542E-13	3.975E-14	5.664E-15	2.147E-16	
63	710	2.083E-12	5.401E-13	1.310E-13	3.344E-14	4.703E-15	1.752E-16	
64	720	1.807E-12	4.636E-13	1.113E-13	2.813E-14	3.906E-15	1.430E-16	
65	730	1.568E-12	3.980E-13	9.450E-14	2.366E-14	3.243E-15	1.167E-16	
66	740	1.360E-12	3.417E-13	8.026E-14	1.991E-14	2.693E-15	9.528E-17	
67	750	1.180E-12	2.933E-13	6.817E-14	1.674E-14	2.237E-15	7.777E-17	
68	760	1.024E-12	2.518E-13	5.791E-14	1.409E-14	1.857E-15	6.347E-17	
69	770	8.883E-13	2.161E-13	4.918E-14	1.185E-14	1.542E-15	5.181E-17	
70	780	7.706E-13	1.855E-13	4.178E-14	9.967E-15	1.281E-15	4.229E-17	
71	790	6.686E-13	1.593E-13	3.548E-14	8.385E-15	1.064E-15	3.451E-17	
72	800	5.800E-13	1.367E-13	3.014E-14	7.053E-15	8.833E-16	2.817E-17	

FIGURE CAPTIONS

1. Values of the normalization constant A as a function of incident proton energy for each angular interval. The smooth curves represent linear fits to the values at 150, 200, and 250 MeV.
2. Values of the slope parameter B as a function of incident proton energy for each angular interval. The smooth curves represent linear fits to the values at 150, 200 and 250 MeV.
3. Values of parameters A and B as a function of angle at 400 MeV. The smooth curves represent fits to the equations shown on each graph.
4. Values of $r^2 \times \text{DOSE}$ for 400 MeV protons as a function of depth R in a concrete shield for the angular intervals shown.
5. Comparison of $r^2 \times \text{DOSE}$ as a function of depth R in a concrete shield at 400 MeV for the SAIC extrapolation with predictions of the Moyer model in each angular interval.

Figure 1

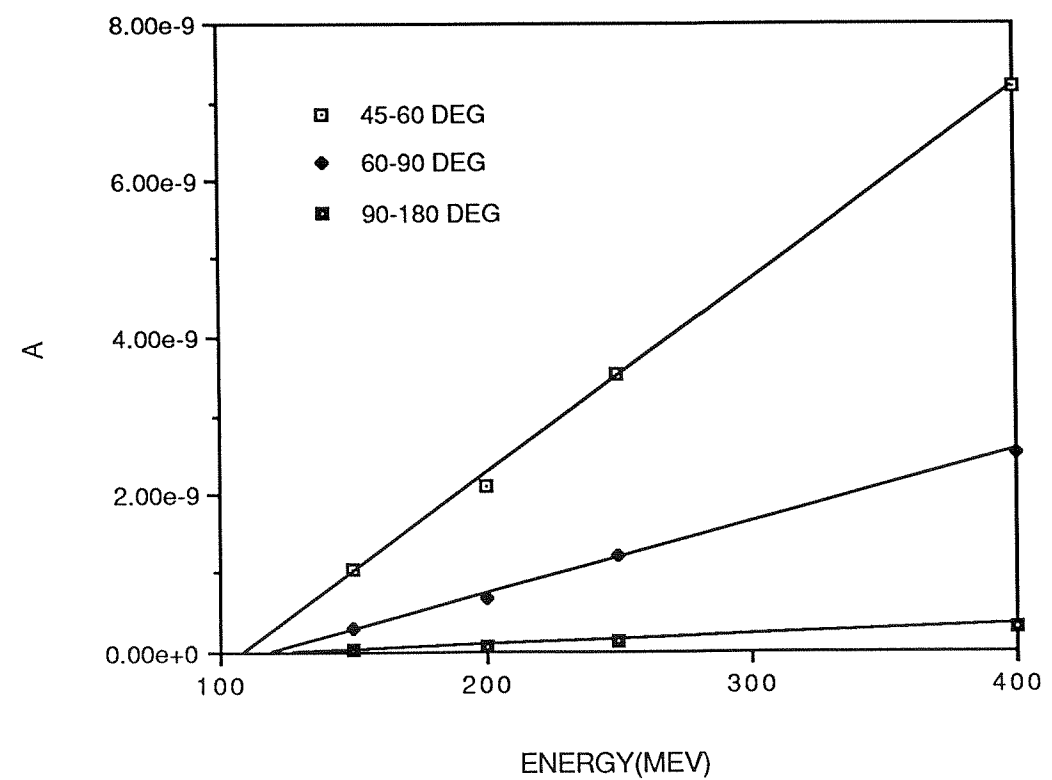
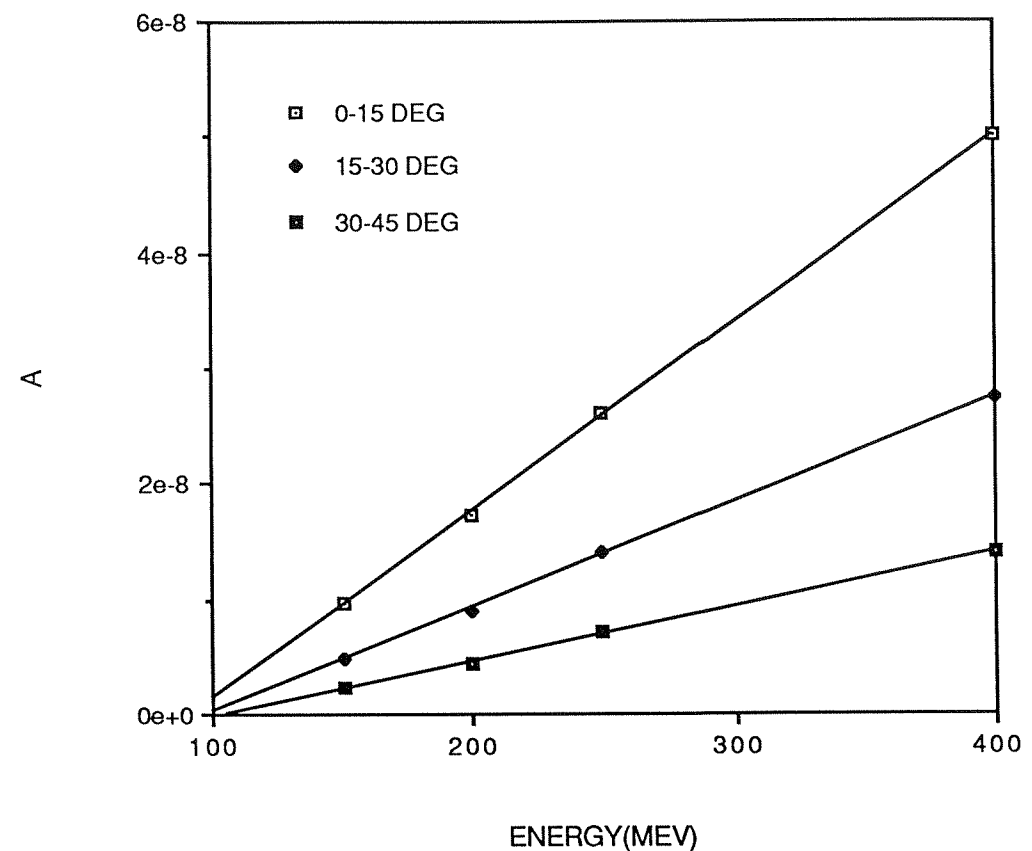


Figure 2

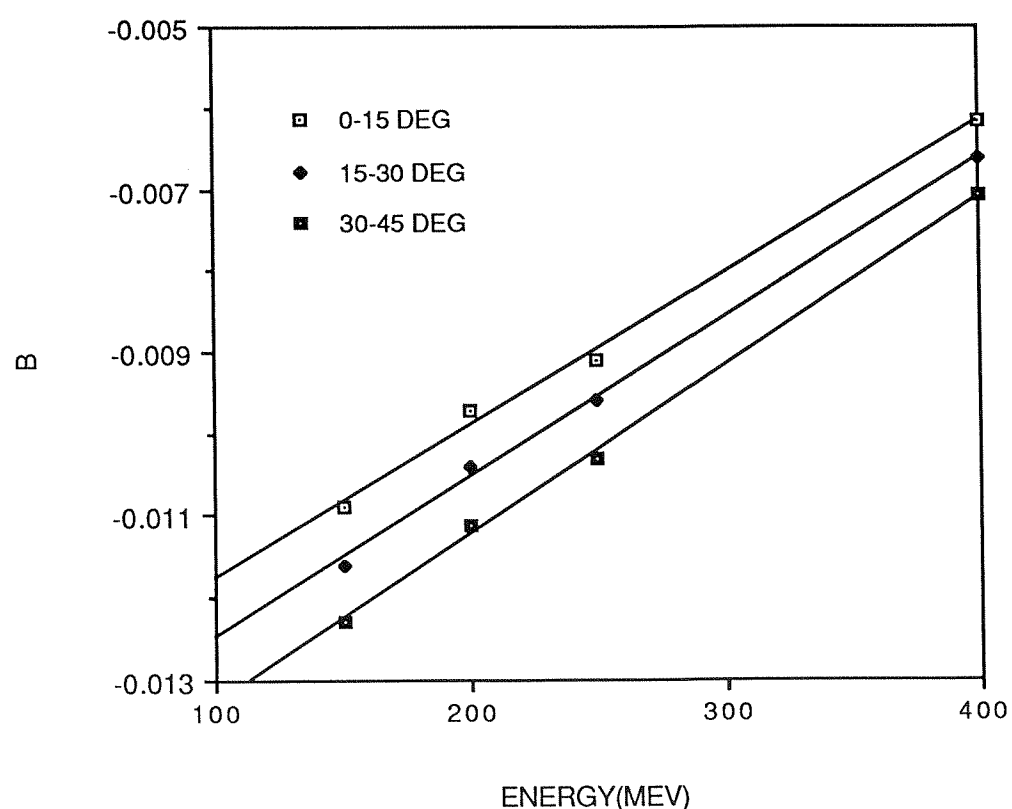
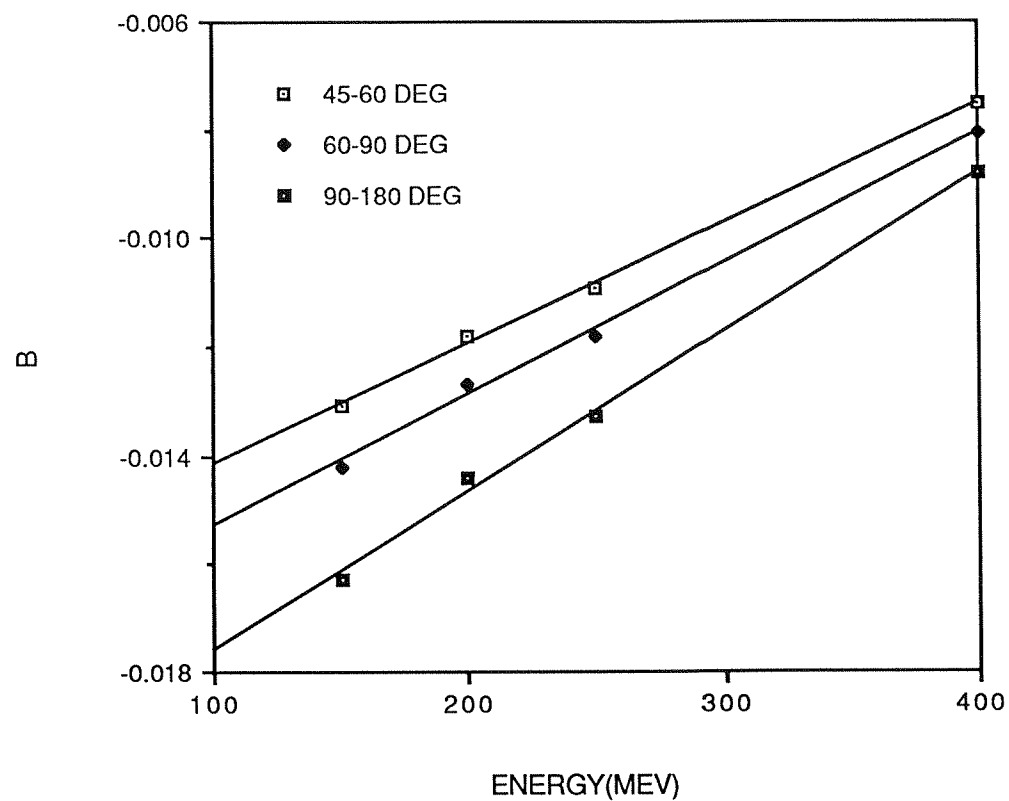


Figure 3

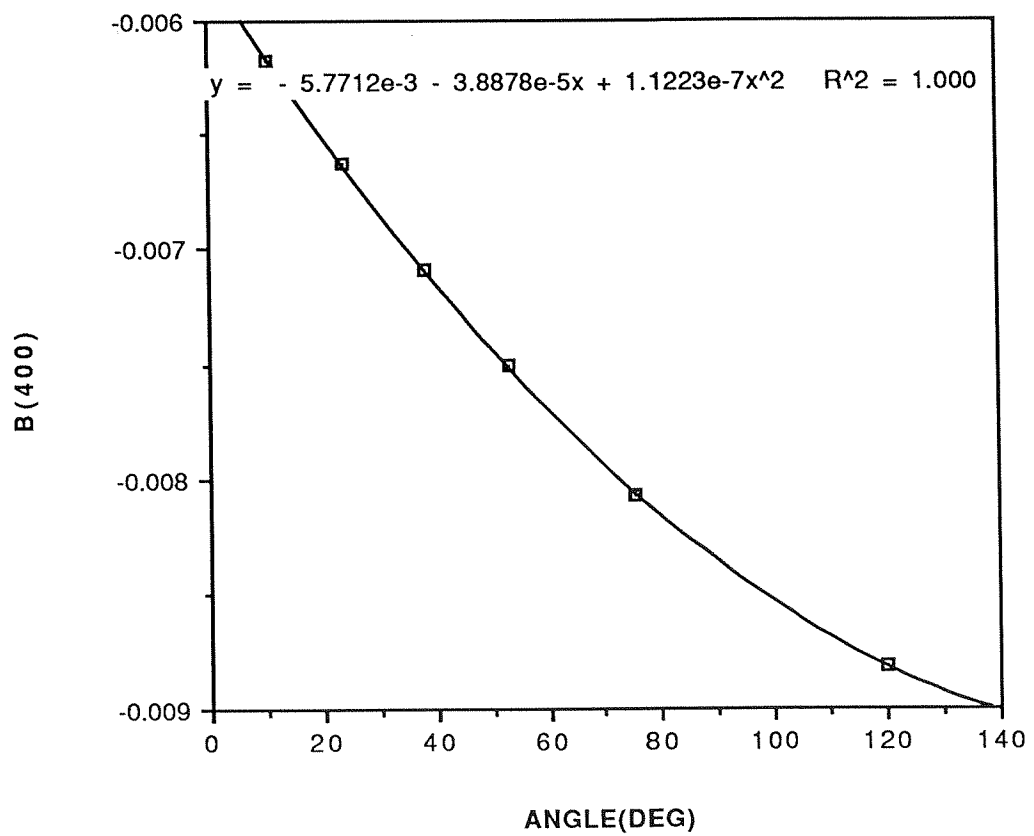
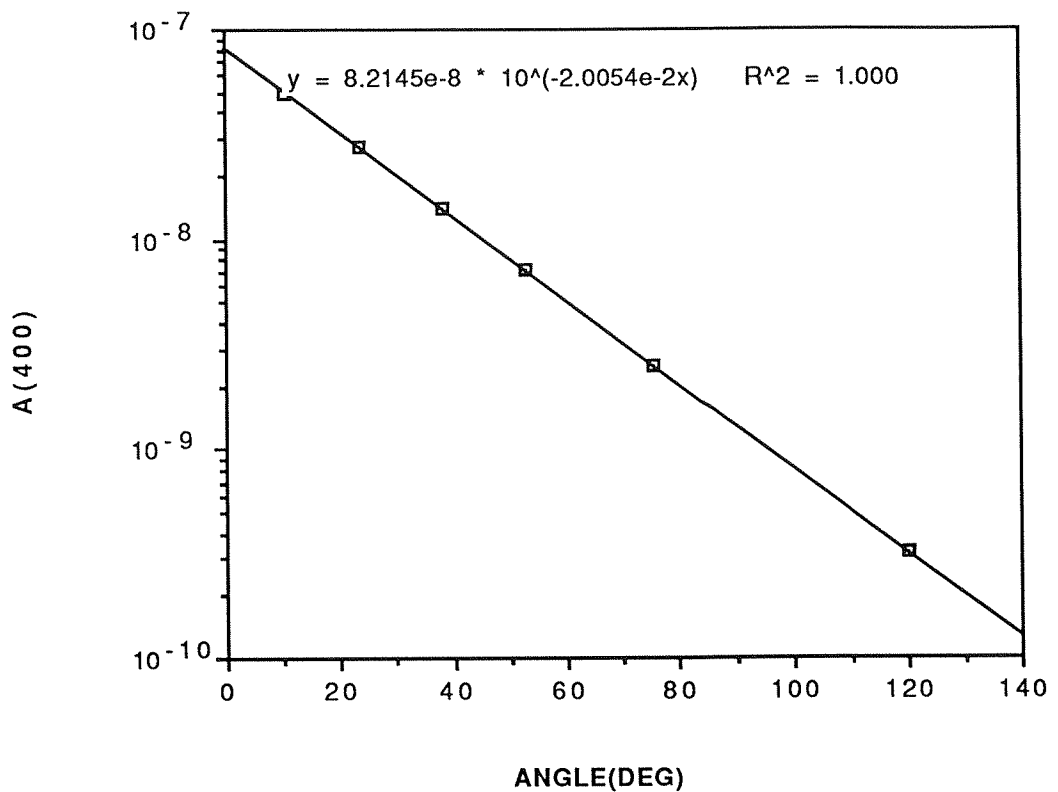


Figure 4

DOSE400.XLC

DOSE EQUIVALENT FOR 400 MEV PROTONS

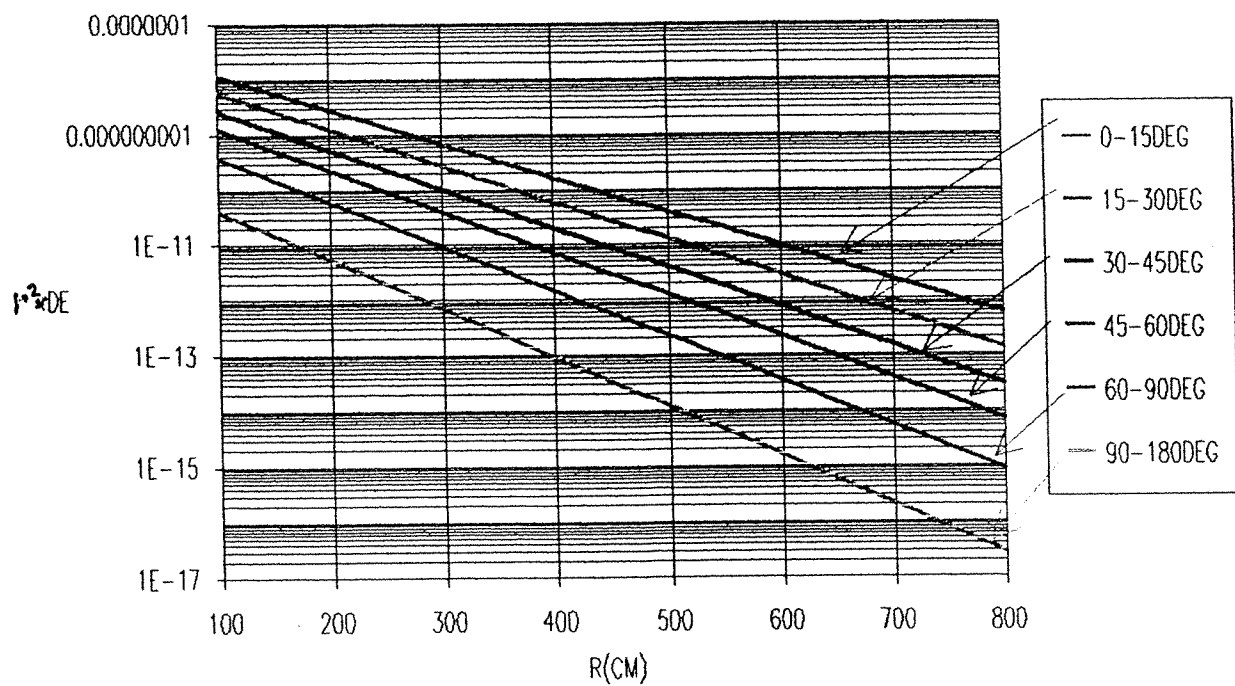


Figure 5

